Quality Assessment of Various CHC NAV GNSS Receiver Models

Zafirah, Z.,[1] Sulaiman, S. A. H.,[1*] Natnan, S. R.,[2] Idris, A. H. M.[3] and Satirapod, C.[4]
[1]School of Geomatics Science and Natural Resources, College of Built Environment, Universiti Teknologi MARA, 40450 Shah Alam, Selangor, Malaysia
E-mail: zafirahzawawi@gmail.com, E-mail: saifulaman@uitm.edu.my*
[2]Bandwork GPS Solutions Sdn Bhd, Unit 9-11, Menara K1, Lorong 3/137C, Old Klang Road,58000, Kuala Lumpur, Malaysia, E-mail: reza@bandwork.com.my
[3]Cadastral Section, Department Survey and Mapping Malaysia, E-mail: ahmadhilmi@jupem.gov.my
[4]Department of Survey Engineering, Faculty of Engineering, Chulalongkorn University, Thailand
**Corresponding Author*

DOI: https://doi.org/10.52939/ijg.v19i5.2655

Abstract
GNSS is utilized in numerous industries and applications to determine a location's (position and time). GNSS technology was quickly used for surveying because it can offer correct latitude, longitude, and height without establishing angles and distances. It's utilized worldwide in mapping and surveying. An ideal GNSS receiver for geodetic and other surveying applications must receive and monitor both code pseudo ranges and carrier phase signals, including the Y-codeless signal. Using geodetic equipment can offer the most accurate location data, but it depends on the instrument's quality. Choosing the proper equipment ensures trustworthy location data. Surveyors may pick cheap equipment caused by financial constraints. Does the data from different GNSS receiver brands have the same quality? By performing static observation on various GNSS receiver from CHC (i90, i83, i80, i73 and i70) key parameters are extracted from the data for data integrity assessment in terms of multipath, cycle slip, signal noise ratio, sky plot and others. CHC Geomatics Office 2 was used to extract the mentioned parameters for quality assessment. The two-day observation lasted from April 23 to April 25, 2022. (GPST). Data availability and data completeness are closely related criteria. For full potential analysis, receivers must be fully operating. No receiver has 100% data completeness or 24-hour data availability. Each receiver's data demonstrates that error varies by parameter. CHC i70 has the least multipath effect and CHC i80 the greatest. Overall, MP1 and MP2 multipath effects were below 0.5. CHC i70 had the lowest cycle slip ratio as it recorded the strongest signal strength while the greatest cycle slip ratio occurred to CHC i80. Each receiver's sky map exhibits the same pattern for both observation days, indicating they tracked the same satellite. Lastly, the average coordinates acquired either on various days or among the receivers indicates a maximum of 0.28m in vector displacement where it is appropriate to claim that each receiver received different coordinates since they were not locating on one place but adjacent within 1 meter radius. From the data analyzed, it is concluded that CHC i83 has best data quality among CHC models while CHC i80 obtained the worst data quality, but this does not indicate that model cannot provide good quality data.

Keywords: CHCNAV, Geodetic, GNSS, Quality Assessment, Surveying

1. Introduction

Global Navigation Satellite System or GNSS is used in many sectors and applications in obtaining the position or navigation of a location. Because it can easily provide exact position, including latitude, longitude, ellipsoidal height and time without the need to establish the angles and distance between different points, GNSS technology was soon adopted for surveying. It is an essential component of mapping and surveying procedures used all over the world. By using geodetic instruments, the highest probable accuracy of the data can be achieved in obtaining position, but it also depends on the quality provided by the instrument itself. There are two major forms of pseudo-range measurements from satellites that GNSS receivers provide which is code and carrier phase measurements. The code measurement is often noisy, and the carrier phase measurement is more exact than the former, however there is an ambiguity problem that arises from carrier tracking cycle slip [1].

An ideal GNSS receiver for geodetic and surveying applications must be able to receive and track both code pseudo ranges and carrier phase signals, including the Y-codeless signal, in order to produce valid data [2]. Nowadays, even smartphone can provide positioning and navigation by using a low-cost GNSS chipsets [3] and [4]. This shows that regular user can use GNSS technology to obtain a position. However, in survey works, high accuracy and precision is required to provide the best data to be used. There are many manufacturers that produced GNSS receiver providing the same aim to offer instrument that can be used to obtain positioning. As GNSS receivers come from various brands, the quality of GNSS data provided from the receivers may be same but may also be different. The brands that usually used are Trimble, Topcon, Leica, CHC, South etc.

A variety of error factors influence the accuracy of GPS positioning. Users must first determine the primary error causes affecting the quality of GPS sensing data in order to acquire high-precision positioning outputs (i.e., GPS observations). Cycle slips, multi-path, quasi-random errors, and atmospheric delays are the major drivers of degradation in GPS data processing that can degrade the quality of observations and, as a result, the accuracy of positioning outputs [5] [6] [7] and [8]. In order to achieve consistent high-precision positioning findings with the GPS carrier-phase analysis, errors that are not defined in a functional or statistical model must be reliably found, eliminated, and managed in data processing. One of the most difficult aspects of GPS data quality control is reliability [9], which refers to the ability to recognize such flaws and foresee the implications on a solution. Since the deployment of GPS/GNSS in life-critical applications, integrity has become a serious problem. This is due to the fact that restricted satellite visibility, noise, multipath effect, and other undesirable limitations such as environmental degradation can drastically reduce GNSS positioning performance [10] and [11]. Integrity is one of the factors used to assess GNSS performance where it measures the confidence in the accuracy of the information provided by the overall process. Integrity is a general performance characteristic that refers to a user's ability to trust the provided value of a specific location or velocity quantity (e.g., horizontal and vertical position) [12] and [13].

2. Problem Statement

GNSS observation is applied in most survey works as it provides the highest accuracy compared to previous method that used EDM equipment such as total stations. As GNSS technology is used widely, there are many manufacturers that offer different types of GNSS receiver models where each may not provide the best data quality for positioning as it still contains errors that need to be reduced. To obtain good quality of data, choosing the right equipment is necessary to ensure that the data is reliable to be used for positioning. But, due to certain budget limit, surveyor may choose low-cost equipment. Based on previous research, it tested one type low-cost GNSS receivers' performance and concludes that low cost receiver can provide good performance as the survey grade receiver, and that their practical application was feasible and reliable [1] [2] [14] and [15]. Since this study is conducted in Malaysia, the brands that is used regularly in survey work or for education purposes are Trimble, Topcon, CHCNAV, Leica, South and others. There are no previous studies on quality assessment for these brands.

Thus, quality assessment is required for these brands to evaluate does the data acquired from various brands of GNSS receiver provide the same data quality or vice versa. Experimentation of various GNSS model is conducted by performing suitable GPS observation method then detection of vital parameters from the data obtained is required for data integrity checking. The quality checking can be done by using free software or commercial such as Spider QC, RTKLIB, CHC Geomatics Office 2, Anubis, etc. [10] and [14].

3. Materials and Methods

3.1 Study Area

This study requires data that is obtained from the GNSS observation. To perform GNSS observation, site selection is important to avoid any obstacles and reduce the error recorded in each observation. The site to be chosen must meet criteria such as 10° - 15° cut-off elevation angle and must be at open space that is far from hazard or obstruction. GNSS receiver must be situated at places where it cannot be disturbed so that observation can be done for a long time. The study area selected is at the Stadium Hoki, UiTM Shah Alam. It is suitable as it is located at open space which will not disturb any passer-by there. Meanwhile, Figure 1 shows the GNSS configuration setup during the observation at the study area.

3.2 Data Collection

Static method is chosen for data collection of this study. For this study, the observation was done for 2 days continuously for all of the instrument simultaneously to see if each model tracks the same error, same data throughout the observation.

Figure 1: GNSS configuration setup

Table 1: Configuration for quality checking in CGO2

Parameters	
Elevation Mask (°)	10
Sample Interval(s)	1
SNR Threshold Check	Checked
Multipath Check	Checked
Threshold	
Maximum Mp1 RMS	0.5
Maximum Mp2 RMS	0.75
Minimum GPS L1 SNR (dB-Hz)	48
Minimum GPS L2 SNR (dB-Hz)	36
Cycle Slip Ratio	400
Data Utilization Rate (%)	95
Constellation	
Use GPS	Checked
Use GLONASS	Checked
Use BEIDOU	Checked
Use GALILIEO	Checked

Each receiver used the same setting during the start of observation, which is 1HZ for sampling interval, 10° for elevation mask, 1440 minutes (24 hours) for logging time and antenna height which differs for every receiver but within 1.600 meter to 1.700 meter. There will be 5 different receivers to be used where only two tripods will be used to set up the receivers. Each 4 of the receivers will be put on a custom-made platform. Throughout the observation, the receivers are monitored every hour to ensure that the observation is continuing. The observation starts at 0000 of 23rd April 2022 until 0000 of 25th April 2022 (GPST). As the logging time maximum is 1440 minutes which is 24 hours, the receivers static setting was relog on 0000 hours of everyday of observation to guarantee that the observation is ongoing.

3.3 GNSS Data Processing

The CHC Geomatics Office 2 software is used for data processing. CGO 2 was chosen because it is a software that supports a variety of positioning modes for GNSS observation in real time and post-processing. It also supports the widely used standard GNSS data format, RINEX format. One of the powerful tools in the CGO 2 is quality checking tool. This tool can be used to evaluate the quality of GNSS observation data. The configuration of the quality check as shown in the Table 1. Then the result is generated in any format such as KML, SHP, DXF, HTML, CSV, PDF, RAW, ASC and TXT.

4. Results and Discussion

4.1 Data Consistency for Each Model

The RINEX data acquired from a station using five different GNSS receiver models for two consecutive days is the method's input, and the GNSS data quality parameters from the various receivers are the method's output. The station receiver is CHC i90, i83, i80, i73 and i70 where the data sampling interval is 1s with an elevation mask of 10°.

CHC Geomatics Office 2 (CGO2) software is used to extract the data quality information such as data completeness, cycle slip ratio, multipath effect and sky plot. The multipath information value displayed only for L1 and L2 frequency, same goes for the signal-to-noise ratio. As for the cycle slip ratio, it shows the ratio of cycle slip obtained from the number of competed observations divided by the number of ionospheric delays. Meanwhile, the sky plot will display the satellite visibility for GPS only where it will focus on the same time of observation for each observation's day which is on 0000 (GPST) on 23rd and 24th April 2022. Table 2 presents the extracted data quality information from the i90 CNCNAV GNSS model. From the Table 2, the utilization rate of observation data is 95% on the first day of observation and 95.6% on the second day of observation.

Overall, there are more satellites with completed observations (100%) on the second day compared to the first day that explains why the data completeness of second day is higher than the first day. Next, for multipath, it shows all obtained less than 0.5m for both frequencies which is acceptable. Even though there is no difference in multipath error of L1 and L2 frequency within the 2 days observation, it can be seen from the report of quality check that the satellites with unpassed value of multipath is different for each day on each frequency. As example, MP1 for both day shows mostly unpassed multipath value occurred on almost all GLONASS satellites with highest value which is 0.78m on R07 for the first day and 0.86m on R17. As for MP2, the unpassed multipath value occurred mostly on GPS and GLONASS satellites with highest value which is 1.34m on G12 for the first day and 1.32m on G09. As for signal-to-noise ratio, the signal strength for the first day and second day only varies around 0.02dB for L1 and 0.04dB for L2. The number of cycle slip ratio for day showing the same value which is 6. From the quality check report, it can be seen that different days shows different cycle slip detected on different satellites. As example, there is no cycle slip detected on G15, R06, R10, R23, C21, C28 on the first day of observation and R06, R10, R23, C11, C27, C41, C46 and C59 on the second day of observation. The results of the sky plot obtained from the i90 CHCNAV GNSS model are depicted in Figure 2.

Table 2: Data quality information for i90 CHCNAV receiver model

i90	23 April	24 April
Total Epochs	85904	86380
Data Completeness	95%	95.6%
Multipath	MP1 – 0.25 MP2 – 0.35	MP1 – 0.25 MP2 – 0.35
SNR	L1 – 42.86 L2 – 44.21	L1 – 42.88 L2 – 44.25
Cycle Slip Ratio	6	6

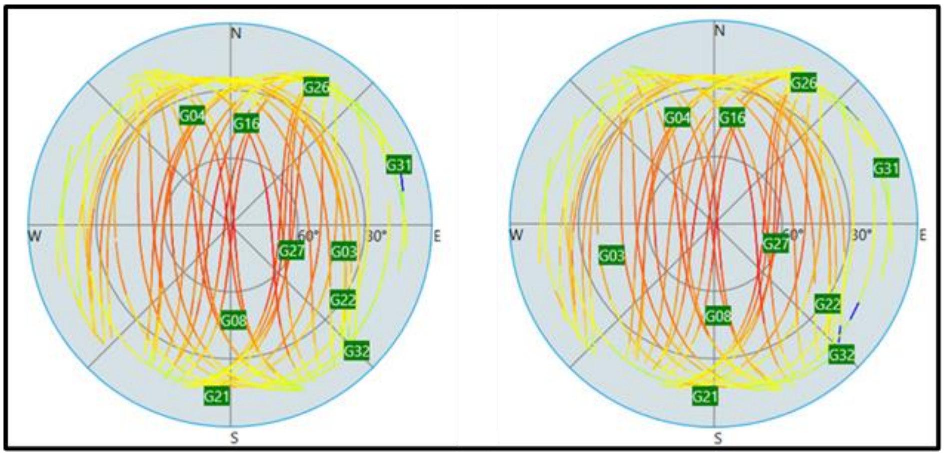

Figure 2: Sky plot for i90 CHCNAV Receiver model on 23 April (left) and 24 April (right)

ISSN: 1686-6576 (Printed) | ISSN 2673-0014 (Online) | © Geoinformatics International

According to the data presented in Figure 2, the quantity of observable satellites remains constant at 10 for each day of observation. The sky plot pattern observed over the course of two consecutive days indicates that the receiver is capable of tracking a specific satellite at identical times, despite the temporal disparity. Figure 3 showing the distribution of single point map for two days. According to Figure 3, the precision of the coordinates and the vector displacement calculated were 0.23m, with discernible differences in pattern between the two figures. The data quality information extracted from the i83 CNCNAV GNSS model is presented in Table 3. From the Table 3, the data completeness of observation is the same for two days which is 95.8%. On the first day, there are more satellites that have finished their observations (100%). In terms of multipath, difference between multipath error for MP1 and MP2 among each day is less than 0.05 m. The difference can be seen with details in the satellites' value of multipath where all passed for GPS, BeiDou and Galileo for both days except on C26 in the second day's MP1. MP1 for both day shows mostly unpassed multipath value occurred on almost all GLONASS satellites with highest value which is 0.83m on R12 for the first day and 0.96m on R02. As for MP2, the unpassed multipath value occurred mostly on GPS satellites with highest value which is 1.45m on G12 for the first day and 1.56m on G09. As for signal-to-noise ratio, the signal strength for each day does not show big differences as it only varies around 0.6dB for L1 and 0.2dB for L2. It appears that the cycle slip ratio for each day is the same, at 6. As they are satellites with 0 complete observation, there is no cycle slip detected on those satellites (R06, R10 and R23). There are other satellites that achieved 0 cycle slip where mostly on BeiDou in the first day of observation and G10, G13, G15 while on the second day cycle slip is undetected on G1, R9, C11, C27, C33, C41, C59.

Figure 4 illustrates the sky plot results derived from the i83 CHCNAV GNSS model. According to the GPS sky plot depicted in Figure 4, the count of observable satellites is consistent at 10 across all days. The uniformity of the celestial chart over the course of two distinct days suggests that the receiver is consistently monitoring a particular satellite at an identical time, despite temporal discrepancies. The distribution of the single point map over a span of 48 hours is depicted in Figure 5 and revealing two discernible patterns for the precision of coordinates. Additionally, the calculated vector displacement measures 0.28m.

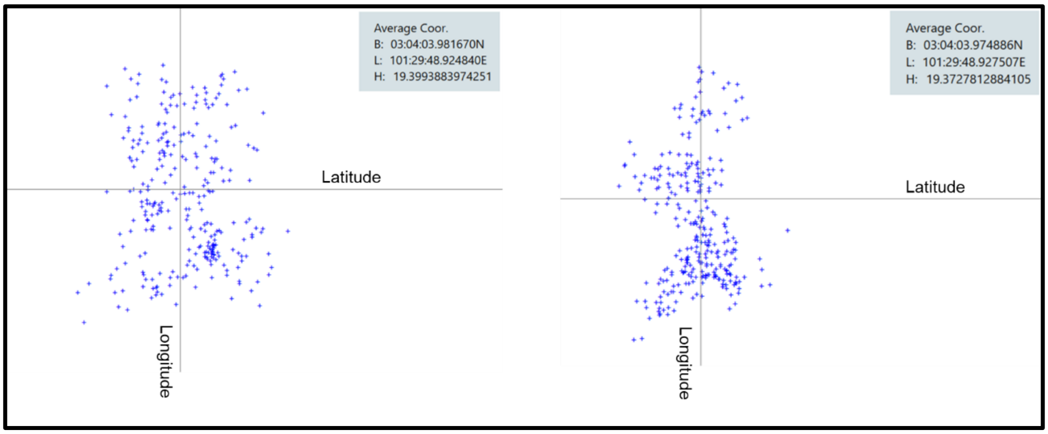

Figure 3: Single point map for i90 CHCNAV Receiver model on 23 April (left) and 24 April (right)

Table 3: Data quality information for i83 CHCNAV Receiver model

i83	23 April	24 April
Total Epochs	86401	86166
Data Completeness	95.8%	95.8%
Multipath	MP1 – 0.23 MP2 – 0.33	MP1 – 0.25 MP2 – 0.36
SNR	L1 – 43.58 L2 – 44.20	L1 – 43.52 L2 – 44.18
Cycle Slip Ratio	6	6

ISSN: 1686-6576 (Printed) | ISSN 2673-0014 (Online) | © Geoinformatics International

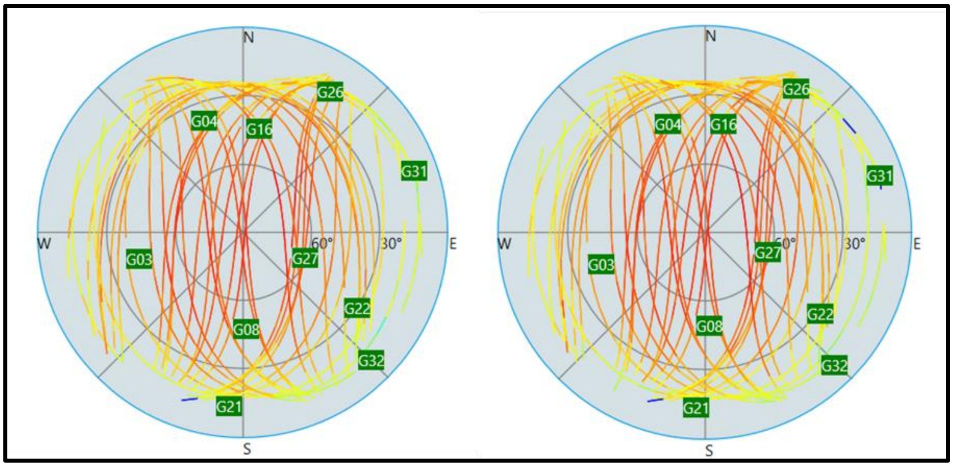

Figure 4: Sky plot for i83 CHCNAV Receiver model on 23 April (left) and 24 April (right)

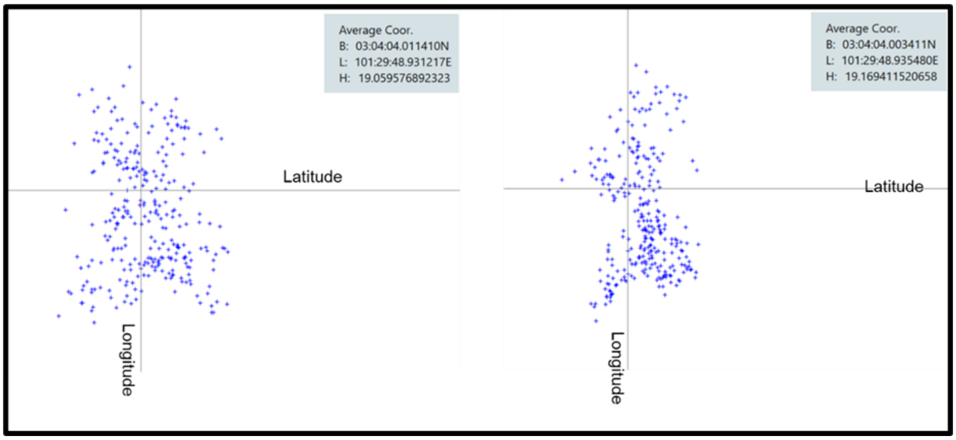

Figure 5: Single point map for i83 CHCNAV Receiver model on 23 April (left) and 24 April (right)

Table 4: Data Quality Information for i80 CHCNAV Receiver model.

i80	23 April	24 April
Total Epochs	86359	83538
Data Completeness	69%	65.9%
Multipath	MP1 – 0.46 MP2 – 0.39	MP1 – 0.46 MP2 – 0.40
SNR	L1 – 42.43 L2 – 41.63	L1 – 42.40 L2 – 41.66
Cycle Slip	3833	490

Table 4 presents the extracted data quality information obtained from the i80 CNCNAV GNSS model. From the Table 4, it can clearly see that the receiver's data completeness does not reach 80% for both days. The value of data completeness for this receiver is highly effected because there is no completed observation on R06, R10, R23, C19 – C30 and all Galileo satellites for both days. There is no data completeness with less than 80% in the satellites of the first day but there are two satellites that does not reach 80% data completeness which is G60 and G20 on the second day. The L1 and L2 frequency suffers the same multipath effects compared with only 0.01m difference between MP2 of both days. Even with small difference, the satellites with unpassed value of multipath is different for each day on each frequency. As example, most unpassed multipath value detected on the MP1 for both days. MP1's highest value is 0.99m on R20 for the first day and 0.84m on R17 for the second day.

As for MP2, there are only few unpassed multipath values where it is detected on G09, G12 on both days and additional of R04 and R24 on the first day of observation. MP2's highest value is 0.83m and 0.84m for first and second day on G12.In terms of signal-to-noise ratio, the signal strength for both L1 and L2 is strong as the value recorded starts from 41dB to 43dB for each day where it only varies about 0.03dB for both frequencies. This receiver shows a big cycle slip ratio for both days where it is 3833 for first day and 490 for second day. The value of cycle slip ratio obtained is large because the percentage of data completeness highly effecting this part. As the number of complete observations is low, combined with the ionospheric delay, the cycle slip ratio will obtain increased. Although the data completeness of first day is better than the second day, the ionospheric delay obtained were low on the first day resulting a high number of cycle slip ratio. The constellation with zero cycle slip detected on the first and second days are the same which is on R06, R09, R23, C19 – C30, all E constellations. The sky plot for i80 shows there is 10 GPS satellites visible on the first and second day as shown in the Figure 6. Figure 7 illustrates the distribution of the single point map across a duration of 48 hours. The observed precision of coordinates depicted in the single point map over a two-day period exhibits a distinct pattern, and there exists a vector displacement of 0.19m between the average coordinates of the two days.

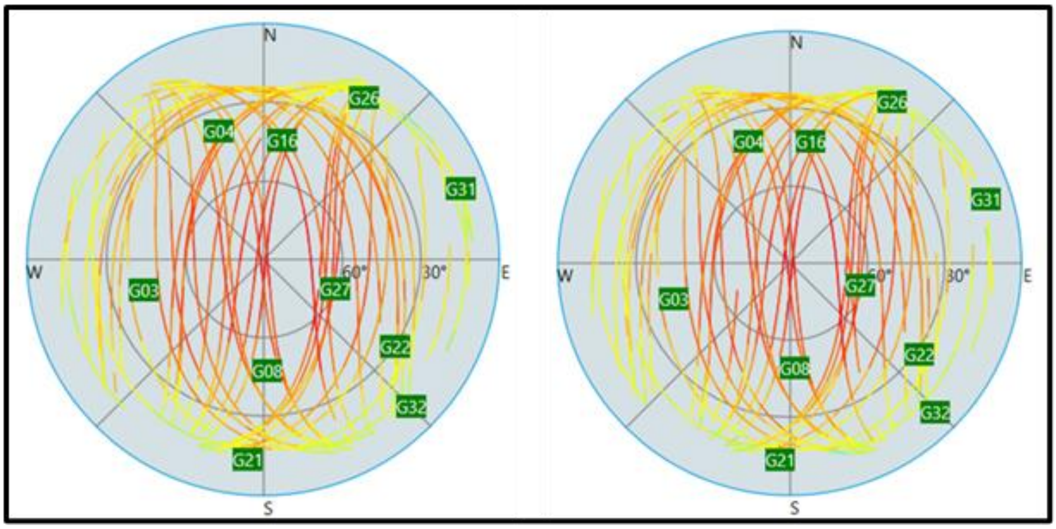

Figure 6: Sky plot for i80 CHCNAV Receiver model on 23 April (left) and 24 April (right)

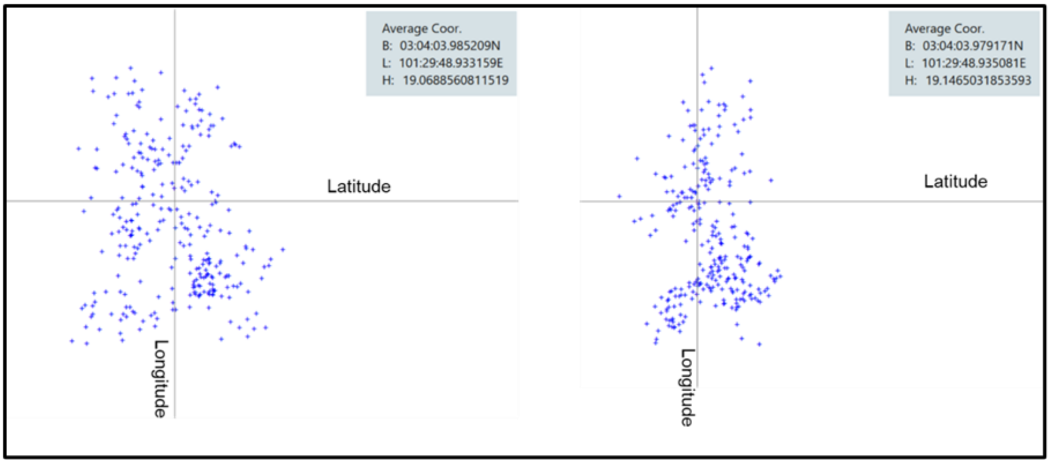

Figure 7: Single point map for i80 CHCNAV Receiver model on 23 April (left) and 24 April (right)

ISSN: 1686-6576 (Printed) | ISSN 2673-0014 (Online) | © Geoinformatics International

The data quality information extracted from the i73 CNCNAV GNSS model is presented in Table 5. Table 5 illustrates that the level of data completeness of the receiver varies on a daily basis. Based on the result, it is still acceptable as it surpasses 80%. On the first day, there are more satellites that have 100% of data completeness than there were on the second day but there are similarities on satellites that does not have any completed observation which is on R06, R10, R23 on both days. There is one different satellite with zero completed observation which is C11 for first day and C14 for second day. The multipath value of both days displays small different. When compared to MP2, the MP1 frequency suffers the least from multipath effects but they only differ around 0.02m maximum for both days. The difference can be seen with details in the satellites' value of multipath where mostly unpassed MP1 occurred on GLONASS satellites with 1.27m as the highest multipath value recorded on R24 for the first day's observation and 1.35m on R05 for the second day. As for MP2, the unpassed multipath value occurred mostly on GPS and GLONASS satellites with highest value which is 1.68m on G12 for the first day and 1.60m on G09. In terms of signal-to-noise ratio, the signal intensity for is approximately around 44dB per day for both L1 and L2 where the value of SNR on L2 is the same for both days. It appears that the cycle slip ratio for each day is the same, at 6. As they are satellites with 0 complete observation, there is no cycle slip detected on R06, R10, R23, C11 and C14. There are more satellites with 0 cycle slip ratio on the first day compared to second day. The satellites involved are C06, C07, C08, C09, C13, C23, C28, C30, C38, C39, C40 for first day and R20, C27, C43 for second day. The graphical representation of satellite visibility (sky plot), exhibits a consistent pattern for the initial and subsequent day. Figure 8 shows graphical representation of satellite visibility during the observation. The data presented in Figure 10 indicates that 10 GPS satellites were successfully tracked on both days. Figure 9 illustrates a noticeable trend in the precision of the coordinates on the individual point map during a 48-hour timeframe. The data presented in the Figure 9 indicates an average coordinate displacement of 0.28 metres.

Table 5: Data Quality Information for i73 CHCNAV Receiver model

i73	23 April	24 April
Total Epochs	86401	86083
Data Completeness	95%	94.7%
Multipath	MP1 – 0.31 MP2 – 0.45	MP1 – 0.33 MP2 – 0.46
SNR	L1 – 43.59 L2 – 43.94	L1 – 43.49 L2 – 43.94
Cycle Slip	6	6

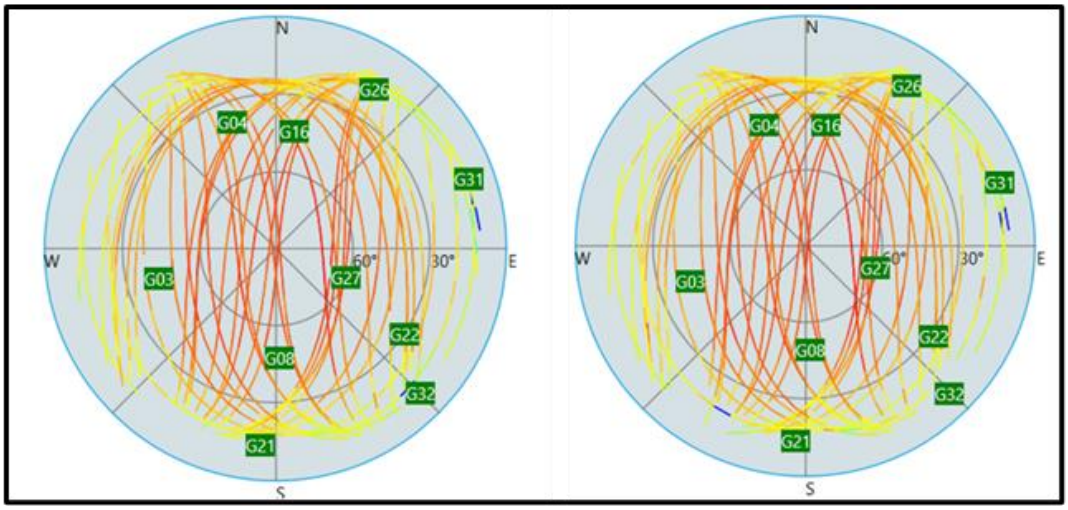

Figure 8: Sky plot for i73 CHCNAV Receiver model on 23 April (left) and 24 April (right)

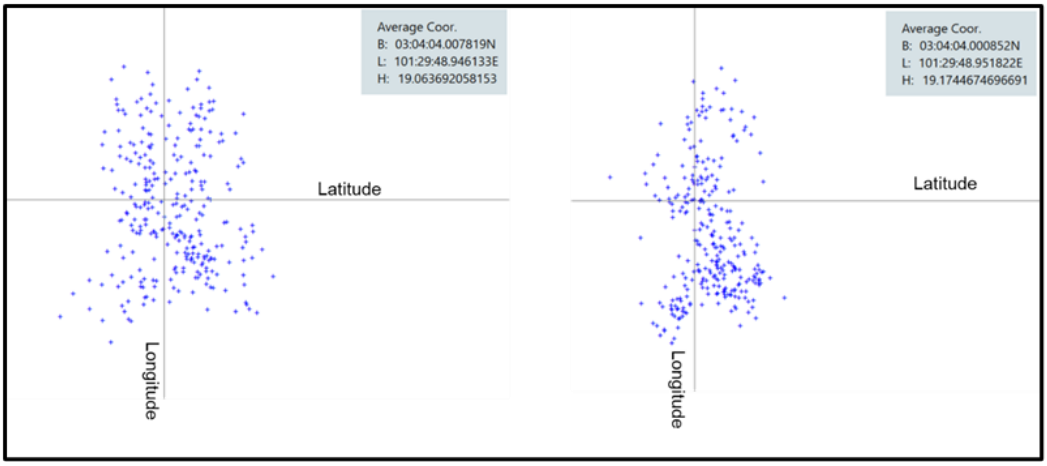

Figure 9: Single point map for i73 CHCNAV Receiver model on 23 April (left) and 24 April (right)

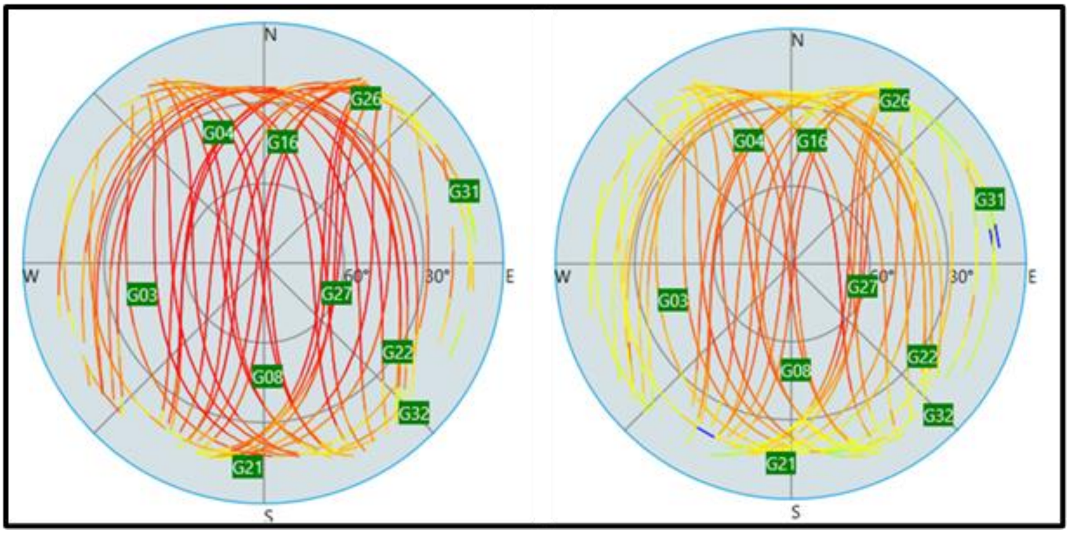

Figure 10: Sky plot for i70 CHCNAV Receiver model on 23 April (left) and 24 April (right)

Table 6: Data Quality Information for i70 CHCNAV Receiver model

i70	23 April	24 April
Total Epochs	86340	86399
Data Completeness	86.9%	87.2%
Multipath (m)	MP1 – 0.14 MP2 – 0.15	MP1 – 0.16 MP2 – 0.20
SNR	L1 – 46.46 L2 – 46.26	L1 – 46.50 L2 – 46.30
Cycle Slip	5	5

Table 6 presents the extracted data quality information derived from the i70 CNCNAV GNSS model. From the Table 6, the data completeness for each day obtained more than 80% which is 86.9% and 87.2% respectively. There are total of 13 satellites (R06, R10, R23 and C21 – C30) that have 0 complete observation which cause the overall data completeness to be reduced on both days. It shows that the multipath is very small and less than 0.5m on both days. Clearly, there is small difference of about 0.02m maximum between the multipath error for L1 while multipath error for L2 differ around 0.05m maximum during the two-day observation period. In the quality check report, there is one unpassed multipath recorded on MP1 of R04 with 0.57m (only on the first day). MP2 only appears unpassed on the second day's observation which is highest on R22 with 1.09m.

In terms of signal-to-noise ratio, the signal intensity of L1 and L2 for each day does not vary that much where the difference between each L1 and L2 is 0.04dB. The cycle slip ratio for each day demonstrates the same value, which is 5. Other than the mentioned satellites that have 0 complete observation earlier, there are other few satellites with 0 cycle slip can be seen such as C01, C02, C03, C05, C06, C07, C09, C10 and C16 for the first day together with G07, C13 and C20 for the second day. The graphical representation of satellite visibility during the observation is depicted in Figure 10. The sky plot pattern depicted in Figure 10 exhibits a consistent trend across each day, with a comparable count of 10 observable satellites on both the initial and subsequent days. Figure 11 displays a discernible trend in the accuracy of the coordinates for the single point map over a span of two days, with an average vector displacement of 0.25m.

4.2 Data Consistency for Each Parameter

The interference between multiple reflected singles and direct GNSS signals received by a receiver's antenna causes multipath error. The reflected signal has a significantly lesser amplitude than the direct signal, and the superposition of the signals causes an interference delay in the received signal, causing the observation value to diverge from the true value. Based on the table above, each GNSS receiver suffers differently in multipath effect even though each receiver is situated at one place where it should obtain the same multipath effect.

Table 7 shows the multipath error for all models. According to the data presented in Table 4, In general, the multipath value for MP1 exhibits a range of 0.14m to 0.46m across both observed days. Notably, the receiver i80 is most significantly impacted by the multipath phenomenon. While for MP2, it starts from 0.15m – 0.46m for both days where the receiver with highest multipath value is i73.

The MP1 and MP2 for i90 and i83 does not show big differences where it differs less than 0.02m for MP1 and less than 0.03m for MP2. Overall, all receivers achieved multipath value less than the threshold stated by IGS where MP1 should be less than 0.5m and MP2 should be less than 0.75m. In conclusion, the highest multipath effect values happen to the i80 while the lowest multipath effect value happen to the i70. There are three main factors that can cause a cycle slip. The first kind is caused by things like trees, buildings, bridges, etc. that block the signal. Second, slips caused by a low signal-to-noise ratio of the measured signal. This is usually caused by multipath, a low satellite elevation, or bad conditions in the atmosphere. Last factor that is uncommon, the third cause of cycle slips is when the receiver software doesn't handle the signal correctly. During the two-day observation, each GNSS receiver should face the same obstruction as it was put in the same location at the same time. The cycle slip ratio shown above is for slips that calculated by dividing the number of complete observations with the ionospheric delay.

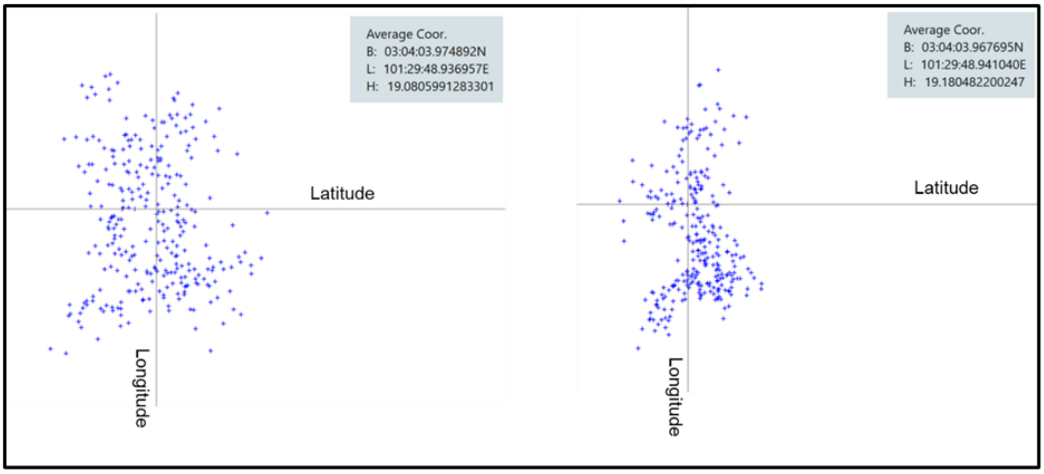

Figure 11: Single point map for i70 CHCNAV Receiver model on 23 April (left) and 24 April (right)

Table 7: Multipath error information during the observation period

	i90		i83		i80		i73		i70	
	MP1	MP2	MP1	MP2	MP1	MP2	MP1	MP2	MP1	MP2
23 April	0.25	0.35	0.23	0.33	0.46	0.39	0.31	0.45	0.14	0.15
24 April	0.25	0.35	0.25	0.36	0.46	0.40	0.33	0.46	0.16	0.20

Table 8: Cycle slip ratio information during the observation period

	i90	i83	i80	i73	i70
23 April	6	6	3833	6	5
24 April	6	6	490	6	5

Table 9: Signal-to-Noise ratio information based on the observation period

	i90		i83		i80		i73		i70	
	L1	L2	L1	L2	L1	L2	L1	L2	L1	L2
23 Apr	42.86	44.21	43.58	44.20	42.43	41.63	43.59	43.94	46.46	46.26
24 Apr	42.88	44.25	43.52	44.18	42.40	41.66	43.49	43.94	46.50	46.30

From the Table 8, it is observed that the maximum value of the cycle slip ratio is 3833 and 490 on the first and second day of observation from i80 and the minimum value is 5 from the i70. All cycle slip ratio is acceptable as it gained less than 10 except for i80 with the worst cycle slip ratio due to the low percentage of data completeness. The other receiver achieved low cycle slip ratio as the value of ionospheric delay is proportional to the number of complete observations. In an electrical equipment or system, the signal-to-noise (SNR) ratio refers to the ratio of signal to noise. There is a difference between signals and noises. Signals are generated by an external device, while noises are made by the equipment itself, and are often accompanied by extra signals (which can also be information). The signal will not change even if the original signal does. Consequently, an increased signal strength corresponds to an elevated ratio of signal to noise. Table 9 displays the signal noise ratio information of each receiver. As per the data presented in the aforementioned table, it can be observed that the signal strength received by each receiver was found to be above 40dB, thereby signifying a robust signal. The Signal-to-Noise Ratio (SNR) values for each model exhibit a range of variability between 41.66dB and 45.50dB. The signal-to-noise ratio (SNR) values obtained by each receiver were found to vary, despite the fact that the L1 and L2 of each receiver exhibited a difference of less than 5dB. The CHC i70 exhibits the highest level of signal strength in comparison to alternative options.

5. Conclusion

It is necessary to check the quality of observation data and use high quality GNSS data for any surveying job to ensure that the data obtained deliver a good set of positionings information. This paper presents a methodology to determine the quality of GNSS observations collected from a station for the purpose of determining either different GNSS receiver obtained the same error and data quality. This method provides a comprehensive set of quality control parameters using the CHC Geomatics Office 2 software. These quality parameters include the number of cycle slips, the multipath effects, the completeness of data, the dilution of precision, satellite geometry, sky plot, average coordinates and the signal strength of data. It is essential that the receivers be run at full capacity in order to thoroughly investigate the full extent of their capabilities. By comparing the results of the data quality checks from five GNSS receiver, it can be seen that each receiver may track different errors even when being put in the same location and run at the same time. But the difference does not differ that much and there is no guideline on what are the acceptable values among different observations. From the data analyzed, it is concluded that CHC i83 has best data quality among CHC models while CHC i80 obtained the worst data quality as the data completeness and number of cycle slip is the worse than others. But this does not indicate that model cannot provide good quality data. With the widespread usage of GNSS applications and the availability of numerous types of GNSS receivers, it becomes increasingly vital to monitor the quality of GNSS observations. The proposed method should be suitable for GNSS users to comprehend those numerous elements affect GNSS data quality, causing each receiver to detect data of varying quality. This will improve users' comprehension of the importance of monitoring discovered faults, which should be minimized by using appropriate software. A wide variety of GNSS applications will be aided by continuous study into the optimal method for leveraging these statistical conclusions and selecting a receiver with high-quality data.

Acknowledgment

The authors acknowledge the assistance provided by Bandwork GPS Solutions Sdn. Bhd. and Shanghai Huace Navigation Technology Ltd in facilitating this research study. The authors express their gratitude towards the anonymous reviewers for their valuable comments that have contributed to the improvement of this manuscript.

References

[1] Zhu, N., Marais, J., Betaille, D. and Berbineau, M., (2018). GNSS Position Integrity in Urban Environments: A Review of Literature. *IEEE Transactions on Intelligent Transportation Systems*, Vol. 19(9). https://doi.org/10.1109/TITS.2017.2766768.

[2] Hofmann-Wellenhof, B., Lichtenegger, H. and Collins, J., (1992) *GPS: Theory and Practice (4th ed.)*. New York: Springer Verlag GmbH.

[3] Janos, D. and Kuras, P., (2021). Evaluation of Low-Cost GNSS Receiver under Demanding Conditions in RTK Network Mode. *Sensors*, Vol. 21(16), http://dx.doi.org/10.3390/s21165552.

[4] Zhang, X., Tao, X., Zhu, F., Shi, X. and Wang, F., (2018). Quality Assessment of GNSS Observations from an Android N Smartphone and Positioning Performance Analysis Using Time-Differenced Filtering Approach. *GPS Solutions*, Vol. 22(3), https://doi.org/10.1007/s10291-018-0736-8.

[5] Guo, L., Jin, C. and Liu, G., (2018). Evaluation on Measurement Performance of Low-Cost GNSS Receivers. *2017 3rd IEEE International Conference on Computer and Communications, ICCC 2017*, *2018-Janua*. https://doi.org/10.1109/CompComm.2017.8322706

[6] Isik, O. K., Hong, J., Petrunin, I. and Tsourdos, A., (2020). Integrity Analysis for GPS-Based Navigation of UAVs in Urban Environment. *Robotics*, Vol. 9(3), 1-20. http://dx.doi.org/10.3390/robotics9030066.

[7] Park, M. and Gao, Y., (2008). Error and Performance Analysis of MEMS-Based Inertial Sensors with a Low-Cost GPS Receiver. *Sensors*, Vol. 8(4). https://doi.org/10.3390/s8042240.

[8] Trajkovski, K. K., Sterle, O. and Stopar, B., (2010). Sturdy Positioning with High Sensitivity GPS Sensors under Adverse Conditions. *Sensors*, Vol. 10(9). https://doi.org/10.3390/s100908332.

[9] Lee, D., Cho, J., Suh, Y., Hwang, J. and Yun, H., (2012). A New Window-Based Program for Quality Control of GPS Sensing Data. *Remote Sensing*, Vol. 4(10), 3168–3183. https://doi.org/10.3390/rs4103168.

[10] Angrisano, A., Dardanelli, G., Innac, A., Pisciotta, A., Pipitone, C. and Gaglione, S., (2020). Performance Assessment of PPP Surveys with Open Source Software Using the GNSS GPS–GLONASS–Galileo Constellations. *Applied Sciences*, Vol. 10(16). http://dx.doi.org/10.3390/app10165420.

[11] Braasch, M. S. and Spilker, B. W., 1996. Multipath Effects. In B. W. Parkinson & J. J. Spilker (Eds.), *Global Positioning System: Theory and Applications.* Washington, DC: AIAA.

[12] Liu, N., Zhang, Q., Zhang, S. and Wu, X., (2021). Algorithm for Real-Time Cycle Slip Detection and Repair for Low Elevation GPS Undifferenced Data in Different Environments. *Remote Sensing*, Vol. 13(11). http://dx.doi.org/10.3390/rs13112078.

[13] Ma, H., Zhao, Q., Verhagen, S., Psychas, D. and Liu, X., (2020). Assessing the Performance of Multi-GNSS PPP-RTK in the Local Area. *Remote Sensing*, Vol. 12(20). http://dx.doi.org/10.3390/rs12203343.

[14] Cutugno, M., Robustelli, U. and Pugliano, G., (2020). Low-Cost GNSS Software Receiver Performance Assessment. *Geosciences*, Vol. 10(2). http://dx.doi.org/10.3390/geosciences10020079.

[15] Ma, X., Yu, K., He, X., Montillet, J. P. and Li, Q., (2020). Positioning Performance Comparison between GPS and BDS with Data Recorded at Four MGEX Stations. *IEEE Access*, Vol. 8, 147422-147438.